ACS APPLIED MATERIALS & INTERFACES

Research Article

www.acsami.org

Upshift of Phase Transition Temperature in Nanostructured $PbTiO_3$ Thick Film for High Temperature Applications

Jungho Ryu,[†] Guifang Han,[†] Tae Kwon Song,[§] Aaron Welsh,[∥] Susan Trolier-McKinstry,[∥] Hongsoo Choi,[⊥] Jong-Pil Lee,[#] Jong-Woo Kim,[†] Woon-Ha Yoon,[†] Jong-Jin Choi,[†] Dong-Soo Park,[†] Cheol-Woo Ahn,[†] Shashank Priya,[▽] Si-Young Choi,*[,‡] and Dae-Yong Jeong*[,○]

[†]Functional Ceramics Group, and [‡]Advanced Characterization & Analysis Group, Korea Institute of Materials Science (KIMS), Changwon 641-831, Korea

[§]Department of Convergence Materials Science and Engineering, Changwon National University, Changwon 641-773, Korea

[∥]Materials Research Institute, The Pennsylvania State University, University Park, Pennsylvania 16802, United States

[⊥]Bio-Micro Robot Lab, Daegu Gyeongbuk Institute of Science and Technology (DGIST), Daegu 711-873, Korea

[#]Department of Materials Science and Engineering, Myongji University, Gyeonggi 449-728, Korea

[▽]Center for Energy Harvesting Materials and Systems (CEHMS), Virginia Tech, Blacksburg, Virginia 24061, United States

[○]School of Materials Engineering, Inha University, Incheon 402-751, Korea

Supporting Information

ABSTRACT: Thick polycrystalline pure $PbTiO_3$ films with nano size grains were synthesized for the first time by aerosol deposition. Annealed 7 μm thick films exhibit well-saturated ferroelectric hysteresis loops with a remanent polarization and coercive field of 35 $\mu C/cm^2$ and 94 kV/cm, respectively. A large-signal effective $d_{33,eff}$ value of >60 pm/V is achieved at room temperature. The measured ferroelectric transition temperature (T_c) of the films ~550 °C is >50 °C higher than the reported values (~490 °C) for $PbTiO_3$ ceramics. First-principles calculations combined with electron energy loss spectroscopy (EELS) and structural analysis indicate that the film is composed of nano size grains with slightly decreased tetragonality. There is no severe off-stoichiometry, but a high compressive in-plane residual stress was observed in the film along with a high transition temperature and piezoelectric response. The ferroelectric characteristics were sustained until 200 °C, providing significant advancement toward realizing high temperature piezoelectric materials.

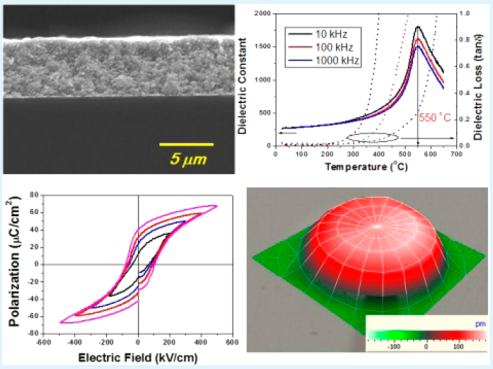

KEYWORDS: *piezoelectric, thick film, $PbTiO_3$, high temperature, aerosol deposition*

1. INTRODUCTION

$PbTiO_3$ (PT) is a prototypical ferroelectric material that serves as one end member for the $Pb(Zr_{1-x}Ti_x)O_3$ (PZT) solid solution.[1−6] PT has a ferroelectric phase transition from a tetragonal structure to a paraelectric cubic one at 493 °C and ambient pressure. This high phase transition temperature (T_c), over 100 °C higher than the morphotropic phase boundary PZT-based piezoelectrics, is attractive for high temperature applications. However, PT has high tetragonality (c/a ratio ~1.06) and experiences a large volume change at the T_c. Thus, the fabrication of crack-free polycrystalline undoped PT ceramics or thick films is exceptionally difficult by any well-established sintering/thick film fabrication route.[1−6] For this reason, there is no report on the successful fabrication of high density pure PTO ceramics or thick films up to date.

The T_c of ferroelectric materials can strongly influence their utility in high temperature sensor and actuator applications. For example, some automobile applications require operating temperatures in the vicinity of 250 °C. Thus, a T_c exceeding 500 °C is highly relevant in this case to avoid depoling and providing low temperature coefficient. As a result, there are ongoing worldwide searches to identify novel high temperature piezoelectric materials.[7]

In addition to the composition, ferroelectric transition temperature can also be displaced by changes in the point defect chemistry or stress in the constituent materials.[8−13] Devonshire's thermodynamic formalism for ferroelectrics reveals that stress is effective in displacing T_c; this prediction has been confirmed by experiments by several research groups.[5,10,14−18] Hydrostatic compressive stresses shift transition temperatures (and sometimes the ferroelectric polymorph) to favor the low volume phase. Likewise, biaxial stresses associated with thin

Received: January 7, 2014
Accepted: July 21, 2014
Published: July 21, 2014

films are widely shown to change T_c. In an early example of this concept, Rossetti et al. reported that for epitaxial PT films on single crystal $SrTiO_3$ substrates, T_c increased relative to the unstressed bulk material because the two-dimensional compressive stress increased the tetragonality.[15] However, in epitaxial PT films under tensile stress with the polarization component along the out-of-plane axis, the tetragonality was decreased and T_c was downshifted. For polycrystalline PT with randomly oriented polarization, three-dimensional (iso-hydrostatic) compressive stresses downshifted T_c.[6,14,17] Prior studies have attributed shifts in transition temperatures to the presence of stress for other sample geometries as well, besides thin/thick films. Yang et al. synthesized high-aspect ratio polycrystalline PT nanotubes and found that T_c shifted to a higher temperature by the in-plane compressive stress present in the nanotubes.[5] These prior experimental results indicate that the residual stress or lead deficiency in perovskite ferroelectric films could both increase the observed T_c value.[11,12] As ceramic PT has a T_c of 493 °C, which is ~100 °C higher than that of PZT, we would expect a T_c of over 500 °C to be achievable by modulation of one or both of these factors.

For actuator applications, as a thin film generates small longitudinal displacement, bending actuators are generally utilized to magnify the displacement. To increase the force generated, thick films are preferable over thin films. Although there have been several reports published on the growth and properties of epitaxial thin PT films, there have been limited studies on stoichiometric polycrystalline thick PT films that exhibit expected ferroelectric and piezoelectric properties. The reason is either limited growth speed or the fact that the processing temperature is higher than T_c, which produces cracks, due to the extremely large volume change during the paraelectric to ferroelectric phase transition. (See Supporting Information S1, as even pure PT ceramics cannot be sintered with high usable high density.)

Aerosol deposition (AD), which is used in this study, is a unique technique that can fabricate dense (relative density of over 96%) polycrystalline thick films with a relatively high deposition rate (over 1 μm/min depending on the deposition area) at room temperature by consolidation of (sub-) micrometer-sized ceramic particles. The deposition mechanism is strongly related to the fracture and plastic deformation of the primary particles.[19−21] AD produces nanosize grains by the collision of highly crystalline particles onto the substrate at high speed; thus, an additional thermal annealing process (for recrystallization and/or grain growth) is also necessary for AD-deposited ferroelectric materials.[21] As described previously, the residual stress of the dense thick film depends on the annealing process.[22] It is plausible that the dense polycrystalline PT thick films could be easily synthesized by AD processes because it can transform the micrometer-sized ceramic powders into dense nanosized crystalline thick films and the in-plane residual stress of the PT film can be controlled by annealing process.

In this Article, highly dense polycrystalline stoichiometric PT thick films on platinized silicon wafer with nanosize grains were produced for the first time by AD. A high T_c caused by residual compressive stress modulation was achieved. Ferroelectric, piezoelectric, and dielectric properties were investigated as a function of temperature. Results were analyzed using a combination of computational modeling, microscopy, and diffraction techniques.

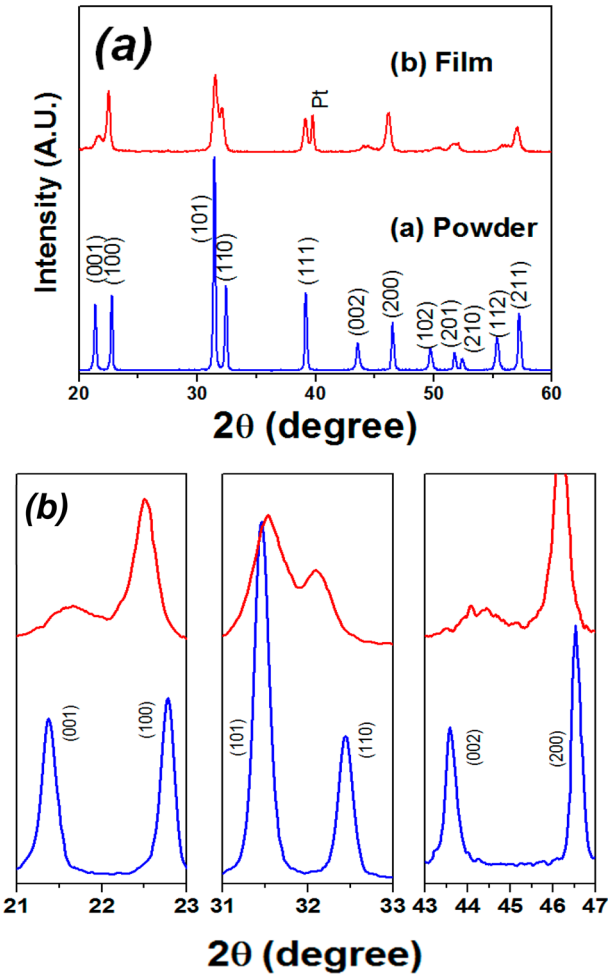

Figure 1. (a) XRD patterns of $PbTiO_3$ powder and the AD film annealed at 700 °C for 1 h and (b) from selected angles. The calcined powder clearly showed a tetragonal structured perovskite phase; excellent crystallinity was also observed for the AD film after annealing. Slight broadness of the peaks as compared to those from powder is due to nanosized grains. The (100) and (200) peaks shifted to lower angles, while the (001) and (002) peaks of AD $PbTiO_3$ were shifted to higher angles, indicative of a slight decrease of c/a ratio.

2. EXPERIMENTAL METHODS

2.1. Film Fabrication. Reagent-grade PbO (99.9+%) and TiO_2 (99.9%) from Aldrich Co., Milwaukee, WI, were used to form $PbTiO_3$ (PT) powder by conventional solid-state reaction at 850 °C for 4 h after 24 h of ball milling. The calcined PT powders were reground to obtain a particle size of $d_{50} \approx 1.5$ μm for the AD process. 3−7 μm thick films were deposited on a Pt-coated silicon wafer [(111) Pt 150 nm/Ti 10 nm/SiO_2 300 nm/Si ⟨100⟩] (from GMek Inc. Gyeonggi, Korea) by controlling the number of scanning cycles at room temperature. The synthesized PT powders were mixed with the carrier gas in the aerosol chamber to form an aerosol flow, which was transported through a tube to a nozzle, accelerated, and ejected from a nozzle with rectangular shaped orifices of 5 × 0.4 mm^2 into a deposition chamber, which was evacuated by a rotary pump with a mechanical booster pump. Medical grade dried air was used as the carrier gas at a flow rate of 5 L/min. The pressures in the aerosol and deposition chambers during deposition were ~600 and ~4 Torr, respectively. The accelerated PT particles collided with the substrate, which was located 5 mm from the nozzle, and formed a dense PT film at room temperature. The linear moving speed of substrate on stage was 1 mm/s. The area of the deposited film was ~5 × 20 mm^2, and the deposition rate was ~1 μm/nozzle scan. The film thickness was

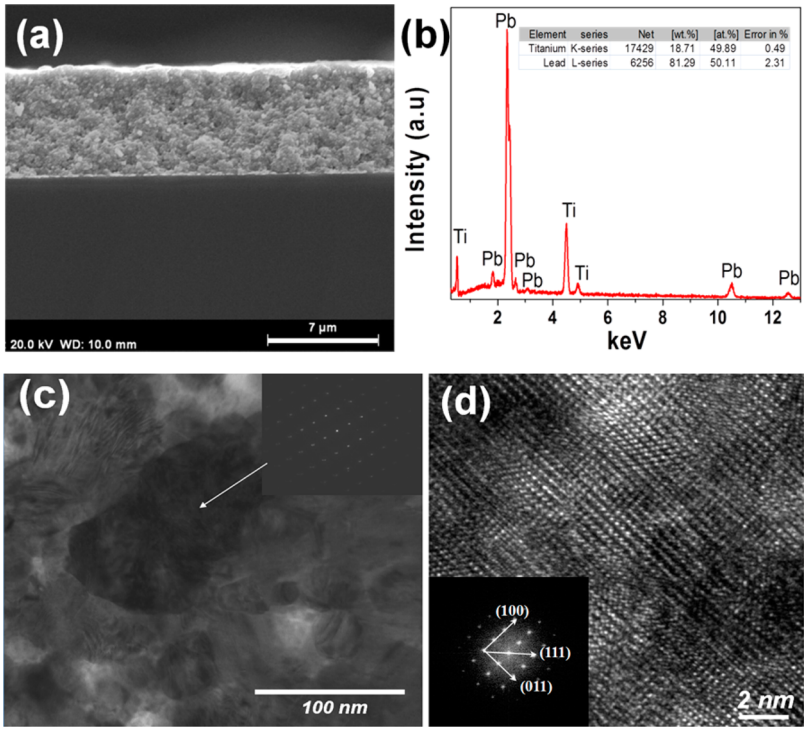

Figure 2. (a) SEM, (b) EDS spectrum and quantitative analysis results, (c) TEM, and (d) HR-TEM images of AD $PbTiO_3$ film annealed at 700 °C for 1 h. The SEM cross-sectional micrograph reveals the soundness of AD PT film even in 7 μm thick films. The EDS results showed that the film has a Pb:Ti ratio of approximately 1:1. The film showed a dense structure with grain sizes ranging from several tens to 150 nm; good crystallinity was confirmed by SAED patterns.

controlled in the range of 3−7 μm by the number of repetitions of the nozzle scan. The films were annealed at 700 °C for 1 h (heating and cooling rate was fixed as 2 °C/min) in air atmosphere without sealing to improve their piezoelectric properties by grain growth or crystallization.

2.2. Crystal Structure, Microstructure, and Defect Analysis. The crystalline phases of the deposited films were identified by X-ray diffractometry. The residual stresses of the films were calculated using the XRD $\sin^2\psi$ method (HR-XRD, X'pert Pro MRD, Philips, Netherlands). Using Cu Kα radiation, a 2θ scan from 54.2° to 59.0° with a step size of 0.03° was used. The psi (ψ) angle was varied from 0° to 50°. The microstructures and composition of the film surface and fracture section were identified by scanning electron microscopy and energy dispersive spectroscopy (SEM and EDS: JSM-5800, JEOL Co., Tokyo, Japan). Electron energy loss spectroscopy (EELS) analysis was conducted to examine the composition of nanosized grain. For this purpose, calculated EELS spectra from first principle modeling were compared to the experimental data from TEM-EELS. The effect of Pb vacancy and O vacancy on the O K edge was computed via CASTEP embedded in Materials Studio (Accelrys inc., U.S.). A 3 × 3 × 4 supercell including a core-hole was constructed, and local density approximation (LDA) was adopted to describe the exchange-correlation functional.

2.3. Dielectric, Ferroelectric, and Piezoelectric Properties. A top Pt electrode with a diameter of ~0.55 mm was sputtered through a metal shadow mask (dot size; ϕ 0.5 mm) to enable measurement of the electromechanical properties. The dielectric properties were obtained using an impedance analyzer (4294A, Agilent Technologies, Santa Clara, CA) from room temperature to 923 K (25−650 °C). The piezoelectric behavior was measured using 3-D laser Doppler vibrometer (LDV, PSV-400 scanning vibrometer, Polytec GmbH, Waldbronn, Germany). A probe tip was contacted to the Pt top electrode so that an AC voltage from 5 to 35 V_{rms} was applied. At each voltage, displacement of the film surface (with/without electroded area) was monitored from over 100 nodes. The driving frequency was 3 kHz, and band-pass filter was applied to minimize noise. The effective piezoelectric coefficient of the structure ($d_{33,eff}$) as a function of driving voltage was calculated from the average displacement value from >30 nodes at plateau. Single beam LDV was applied to double check the measured displacement, and the values were identical to each other (Supporting Information S2). It is possible that the $d_{33,eff}$ values are inflated due to flexure of the sample during field application. The polarization−electric field hysteresis loops were measured by a ferroelectric test system (P-LC100-K, Radiant Technologies, Albuquerque, NM) at 100 Hz from room temperature to 250 °C.

3. RESULTS AND DISCUSSION

Highly dense PT thick films were successfully fabricated without cracks thanks to the advantages of the AD process. To characterize the crystal structure of AD PT films, the X-ray diffraction (XRD) patterns of the calcined powder and AD film annealed at 700 °C for 1 h are compared in Figure 1. The calcined powder showed a tetragonal perovskite phase. Excellent crystallinity was observed in the AD film after annealing. The intensities of the {001} family peaks of the film were lower than those of a random powder pattern. In addition, the (h00) peaks and the (00l) peaks were shifted to lower and higher angles, respectively, indicative of a slight decrease of the c/a ratio. This decrease of tetragonality might be related to the small grain size, a change in defect chemistry, and/or stress in the polycrystalline AD films. Safari et al. have predicted a decrease in the tetragonal phase stability with decreasing particle size in PT.[4] There are several other experimental and theoretical studies reported in the literature that describe the decrease of tetragonality and T_c below a threshold grain size (on the order of 30−80 nm) for perovskite ferroelectrics including PT.[23−26]

The surface, cross-section microstructure, energy dispersive spectroscopy (EDS), and transmission electron microscopy

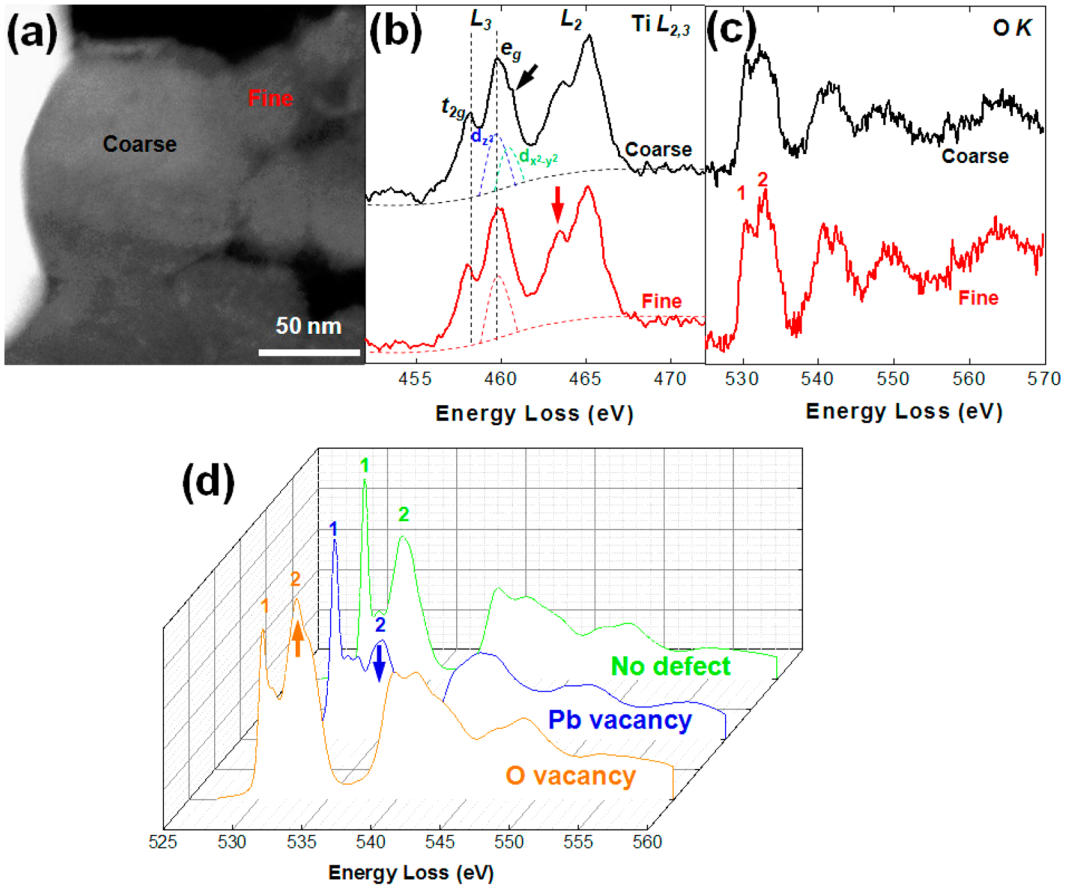

Figure 3. (a) Dark field scanning transmission electron microscopy (STEM) image of the AD $PbTiO_3$ film. EELS spectra of (b) Ti-$L_{2,3}$ and (c) O K edges recorded from fine or coarse grain. (d) Calculated O K edges via the first principle modeling. The EELS spectrum and the first principle modeling analysis results confirm that AD $PbTiO_3$ film does not severely include the lead or oxygen vacancies and also partially exhibits the nanosized grains with a weak tetragonality, together with a few tens to hundred nanometric, tetragonal grains.

(TEM) observations of the films annealed at 700 °C are shown in Figure 2. The polycrystalline AD film adhered well to the Pt bottom electrode without any cracks or delamination, even in the case of 7 μm thick films (as shown in Figure 2a and Figures S2 and S3 in the Supporting Information). The EDS results showed that the film has a Pb:Ti ratio of approximately 1:1. Furthermore, the films showed a dense structure with grain sizes below 150 nm. The crystallinity of the film was confirmed by using selected area electron diffraction (SAED) patterns.

Figure 3a shows the dark field scanning transmission electron microscopy (STEM) image of the fabricated PT film, which exhibits nanosized grains, ranging from ~20 to 150 nm. A smaller grain size will influence the tetragonality, in line with the XRD observations. To clarify the decreased tetragonality in a nanosized grain, electron energy loss spectroscopy (EELS) analysis was conducted; the Ti $L_{2,3}$ edge is sensitive to the change in the tetragonality of perovskite oxides.[27−30] Figure 3b shows the EELS spectra of Ti L edges recorded from coarse and fine grains of Figure 3a. It was found that a decrease in grain size leads to an increase in the L_3 edge splitting (ΔL_3) between e_g and t_{2g} peaks from 1.6 eV in the coarse-grain to 1.8 eV in the fine-grain sample. In the fine-grained sample, according to the crystal-field splitting, the increased (ΔL_3), more symmetric peak in Ti L_3-e_g and the stronger Ti L_2-t_{2g} peak (indicated by the red arrow in Figure 3b) imply that Ti cations are close to the center of the unit cell. Thus, the deceased tetragonality can be directly confirmed via the Ti L edge structure. In the case of the coarse-grained sample, the Ti L_3 e_g peak is broadened, giving rise to an asymmetric peak (indicated by the black arrow in Figure 3b). This occurs as a result of the splitting of Ti L_3 e_g into two different energy levels for the d_{z^2} and $d_{x^2-y^2}$ orbitals.

The Ti L edge also provides information on atomic defects such as Pb and/or O vacancies. To separate these effects, the O K edge structures were also analyzed. The O K edge is strongly affected by the hybridization of the Pb 6sp and O 2p orbitals. In particular, the second peak in the O K edge is sensitively affected by the bonding state between the oxygen and the surrounding cations.[31,32] Figure 3c shows that there are modest differences in the O K edge structures between the coarse and fine-grain films and that both of them are similar to the previously reported O K edge.[29,33]

To validate the effect of Pb vacancy and O vacancy on O K edge, the O K edge was computed via CASTEP embedded in Materials Studio (Accelrys inc., U.S.). A 3 × 3 × 4 supercell including a core-hole was constructed, and a local density approximation (LDA) was adopted to describe the exchange-correlation function. The calculated O K edges are shown in Figure 3d; the green, blue, and orange spectra correspond to the O K edges of defect free, Pb vacancy-containing, and O vacancy-containing supercells, respectively. The calculated O K edge clearly shows that the second peaks are significantly changed by introducing defects; it was observed that the second peaks are noticeably weakened (or strengthened) by the Pb

vacancy (or O vacancy), respectively. By comparing the experimental and calculated O K edge, it seems that the PT film has at most a modest concentration of Pb vacancies and a higher amount of O vacancies. However, the Ti L edges clearly exhibit t_{2g} peaks, suggesting that the film cannot be too strongly oxygen deficient. The generation of oxygen vacancies decreases the valence state of the Ti; in response, the t_{2g} peak is weakened via diminished ΔL_2 and ΔL_3.[34,35] Therefore, the TEM and EELS analysis confirms that the PT film is not grossly nonstoichiometric. The films exhibit a combination of nanosized grains with weak tetragonality, together with tetragonal grains of a few tens to hundreds of nanometers.

To determine the T_c of the AD film, the dielectric constant and loss were measured as a function of temperature as shown in Figure 4a. The AD PT film showed a frequency-independent

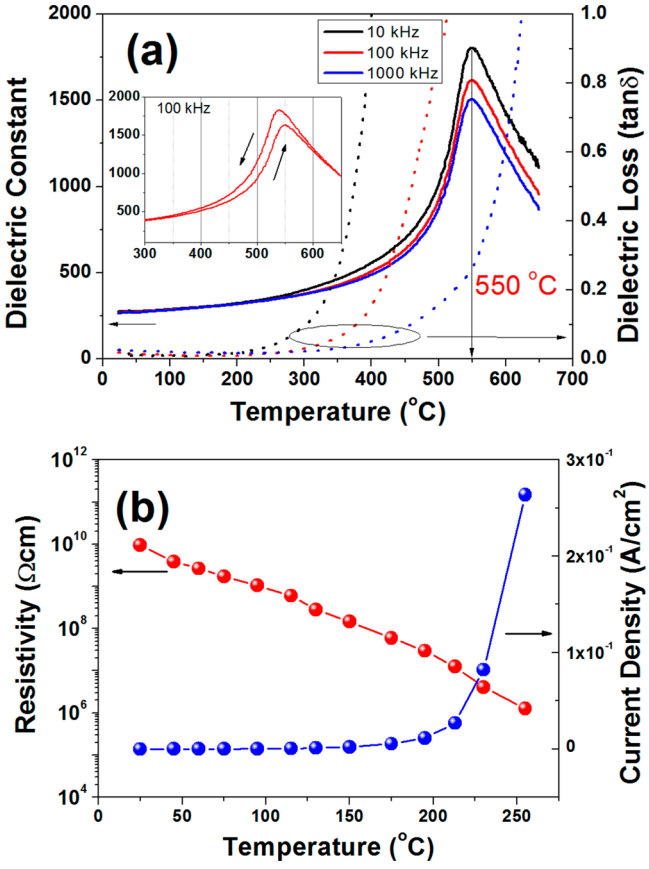

Figure 4. (a) Dielectric constant and loss and (b) resistivity and leakage current density of the AD $PbTiO_3$ film annealed at 700 °C according to the ambient temperature change. Inset in (a) shows T_c difference during heat-up and cool-down. The AD $PbTiO_3$ film showed a frequency-independent T_c characteristic of a normal ferroelectric and a broad permittivity maximum characteristic of a small grained ferroelectrics. The phase transition temperature from the tetragonal to cubic phase (measured on heating) was determined to be ~550 °C, while that measured on cooling was ~535 °C. The dielectric loss, which is an important parameter to estimate the maximum operation temperature of the film, remained below 0.04 up to 250 °C.

T_c characteristic of a normal ferroelectric and a broad permittivity maximum characteristic of a small grained ferroelectric.[36] The phase transition temperature from the tetragonal to cubic phase (measured on heating) was determined to be ~550 °C, which is >50 °C higher than that of PT crystal (493 °C), while that measured on cooling was ~535 °C as shown in the inset of Figure 4a. Furthermore, the dielectric loss tangent, which is an important parameter to estimate the maximum operation temperature of the film, remained below 0.04 up to 250 °C in the measured frequency range. Figure 4b also illustrates resistivity and leakage current density of the PT thick films annealed at 700 °C. The resistivity exceeds 1 MΩ cm below 220 °C. These results are encouraging for high temperature applications, such as automobile applications.[7,37]

Prior studies have shown that T_c can be shifted to higher temperature in the presence of compressive in-plane stress or stoichiometry change.[5,8−18] Because the annealing temperature of the film was 700 °C, it is anticipated that the Pb vaporization should be modest, which is consistent with the results seen in Figures 2 and 3. Therefore, it is plausible that the displacement of the T_c in the AD PT film was mainly caused by residual stress. To assess this hypothesis, the stress in the AD film was evaluated by using the XRD $\sin^2 \psi$ method. The results are depicted in Figure 5. The two-dimensional in-plane stress of the

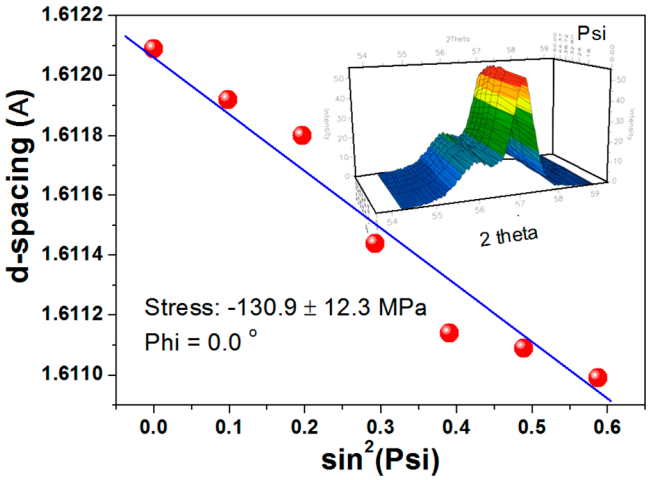

Figure 5. Stress analysis based on *d*-spacing with different ψ orientations of the AD $PbTiO_3$ film annealed at 700 °C by high-resolution XRD $\sin^2 \psi$ method. The two-dimensional in-plane stress of the AD $PbTiO_3$ film was calculated to be −131 ± 12 MPa (compressive stress). This compressive stress is induced during the cooling stage after the thermal annealing process because of thermal expansion coefficient mismatch between substrate and $PbTiO_3$ film. It is believed that the upshift of T_c of $PbTiO_3$ film was mainly affected by this high compressive residual stress in the film.

AD PT film was calculated to be −131 ± 12 MPa (compressive stress). It is possible that this compressive stress is induced during the cooling stage after the thermal annealing process. The Si substrate has a thermal expansion coefficient of 2.62 × 10^{-6}/K to 4.4 × 10^{-6}/K in the temperature range between 25 and 700 °C.[38] However, PT has three distinct stages: above T_c, at T_c, and below T_c.[39−41] Above T_c, polycrystalline PT has a positive thermal expansion coefficient of 35.5 × 10^{-6}/K. At T_c, PT undergoes the phase transition, where the development of the ferroelectric phase introduces a volume expansion of the lattice.[1,40] Below T_c, polycrystalline PT has a negative thermal expansion coefficient of 16.2 × 10^{-6}/K, due to the temperature dependence of the spontaneous strain.[40,41] When the total dimension changes of the Si substrate and the polycrystalline PT during the cooling process from 700 to 25 °C are compared, it is found that the Si substrate shrank more than the PT film, inducing the compressive stress in PT film. It is known that when PZT is grown on single-crystal substrates with larger

dx.doi.org/10.1021/am5000307 | ACS Appl. Mater. Interfaces 2014, 6, 11980−11987

thermal expansion coefficients than the PZT, the resulting compressive stress can increase both the tetragonality and the T_c.[15,42] It is worth noting that the comparatively smaller (h00) peak intensities, as compared to (00k) peak intensities in the films, argues against stress being the only important factor. In contrast, nano size PT powder under free or hydrostatic stress showed the decrease of tetragonality and downshift of T_c.[4] Thus, it is likely that the upshift of T_c was affected by both the stress in the film and potentially a small amount of non-stoichiometry. Because ELLS data and first principal modeling show that our film does not have serious oxygen vacancies, the compressive stress may hinder the dipole to rotate and give rise to the T_c. Rosetti et al. analytically modeled the transition temperature change of PT thin film under stress by using Devonshire thermodynamic formalism.[15] The T_c change in perovskite ferroelectrics can be expressed as in the following equation:[15]

$$\Delta T = T' - T_o = 2\varepsilon_o C(Q_{11}\sigma_3 + 2Q_{12}\sigma_1)$$

where C is the Curie constant, T_o is the Curie–Weiss temperature, σ_1 and σ_3 are the diagonal terms of the stress tensor, and Q_{11} and Q_{12} are the relevant electrostrictive constants in polarization notation. This equation can give us the information that applied/residual stresses renormalize the first-order transition temperature.[6] The stresses σ_1 and σ_3 include the in-plane stress between the film and the substrate, and the hydrostatic pressure resulting from the clamping of grains. Rossetti et al. have shown that the two-dimensional compressive stress results in an increase of transition temperature, while the hydrostatic three-dimensional stresses decrease the transition temperature.[6,15]

The polarization and electric field (P–E) hysteresis loops of the films annealed at 700 °C are shown in Figure 6. Typical

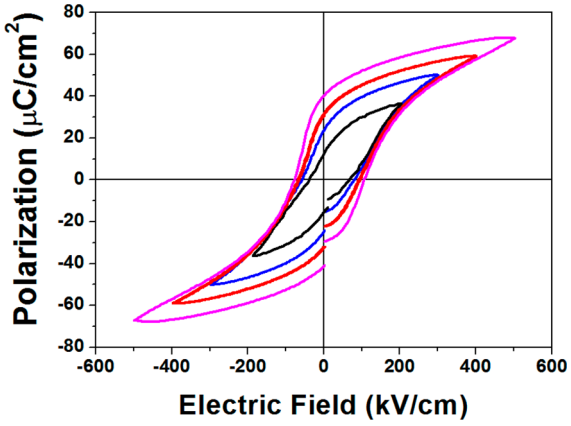

Figure 6. Room-temperature ferroelectric polarization–electric field (P–E) hysteresis loop (at 100 Hz) of the AD $PbTiO_3$ film annealed at 700 °C. It shows typical symmetric and saturated ferroelectric P–E loops, and the remanent polarization (P_r) and coercive field (E_c) were measured to be 35 μC/cm^2 and 94 kV/cm, respectively. These values are comparable to or higher than those obtained from PZT thick films by the AD process.

ferroelectric behavior is demonstrated; the remanent polarization and coercive field were measured to be 35 μC/cm^2 and 94 kV/cm, respectively. These values are comparable to or higher than those obtained from PZT thick films grown by the AD process.[22] The shape of the P–E hysteresis loop confirms ferroelectricity and good breakdown strength in the AD PT film after thermal annealing for grain growth/crystallization. It is also encouraging that the film was not cracked following the polarization reversal.

To investigate its potential use in piezoelectric applications, the effective piezoelectric coefficients of the structure (film and substrate) were measured by three-dimensional laser Doppler vibrometry (3D-LDV).[43] The measurement was achieved by applying an AC electric voltage in the range from 5 to 30 V_{rms} on the top electroded area of the film and recording the 3-D piezoelectric displacement signal from the films. The results are shown in Figure 7, and captured animations of three different

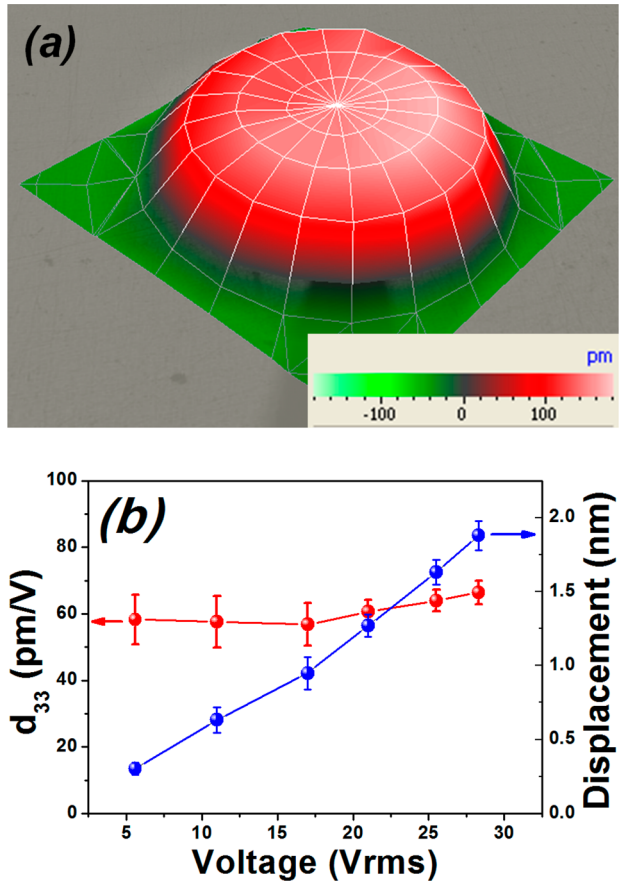

Figure 7. (a) 3-D response while the film expands from three-dimensional LDV scanning of the piezoelectric displacement responses of the AD $PbTiO_3$ film annealed at 700 °C and (b) the effective piezoelectric coefficient $d_{33,eff}$ and displacement as a function of applied voltage. A 3 kHz 5.7 V_{rms} AC voltage was applied on the film via a probe. The error bars in (a) represent the average of 30 individual node values at the deformed crest. From this displacement versus applied voltage plot, the effective piezoelectric coefficient (~60 pm/V) was calculated from the slope, and this value is comparable to that of PZT films fabricated by the AD process.[22]

electric field-induced deformations are provided in Supporting Information S3. Each data point in Figure 7a represents an average of 30 individual node values at the deformed crest. The displacement as a function of applied voltage showed a linear increase over the applied voltage (Figure 7b), which corresponds with the typical piezoelectric behavior. From this displacement versus applied voltage plot, the effective piezoelectric coefficient (~60 pm/V) was calculated from the slope; this value is comparable to that of PZT films fabricated by the AD process.[22]

To clarify the ferroelectric property changes with ambient temperature, the ferroelectric P–E hysteresis of the PT film was

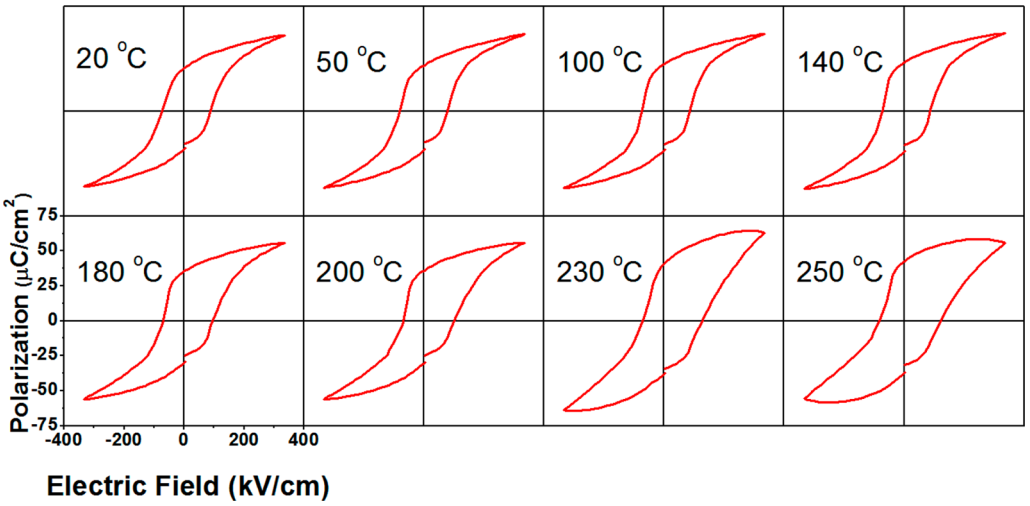

Figure 8. Ferroelectric polarization−electric field (P−E) hysteresis curve of the AD $PbTiO_3$ film annealed at 700 °C with temperature change. The film showed relatively stable P−E loops up to 200 °C without significant changes in remnant/saturated polarization (P_r/P_s) and coercive field (E_c) of typical symmetric and saturated P−E ferroelectric hysteresis loop with respect to temperature.

evaluated as a function of temperature; the results are depicted in Figure 8. The PT films fabricated in this study showed relatively stable P−E loops up to 200 °C without significant changes in remanent/saturation polarization (P_r/P_{sat}) and coercive field (E_c). The result is consistent with the dielectric properties and leakage current data as a function of temperature as shown in Figure 4.

4. CONCLUSION

Dense nanocrystalline thick $PbTiO_3$ films were successfully fabricated for the first time by AD at room temperature. Films annealed at 700 °C for 1 h exhibited a smaller tetragonality than bulk PT, but with clear ferroelectric behavior. The remanent polarization and coercive field were 35 $\mu C/cm^2$ and 94 kV/cm, respectively. The effective structure piezoelectric coefficient was measured to be >60 pm/V. Furthermore, the T_c of the PT film was 550 °C, which is >50 °C higher than that of bulk PT ceramics. The decrease of tetragonality was explained with nano sized grains, while the upshift of T_c was attributed to a combination of the internal in-plane compressive stress and some nonstoichiometry. It is expected that AD PT properties are promising for extending the role of piezoelectrics in high temperature applications.

■ ASSOCIATED CONTENT

Ⓢ Supporting Information

Photo of pure sintered PT ceramics, SEM images of PT film, photo and optical micrograph of PT film, $d_{33,eff}$ measurement data from single beam LDV, animation of piezo-response deformation at 5.7, 11, and 17 V_{rms}, captured images of animation at 5.7 V_{rms}, and plot of inverse dielectric susceptibility as a function of temperature. This material is available free of charge via the Internet at http://pubs.acs.org.

■ AUTHOR INFORMATION

Corresponding Authors

*E-mail: youngchoi@kims.re.kr.

*Phone: + 82-32-860-7548. Fax: +82-32-862-5546. E-mail: dyjeong@inha.ac.kr.

Notes

The authors declare no competing financial interest.

■ ACKNOWLEDGMENTS

This research was supported by the Basic Science Research Program through the National Research Foundation of Korea (NRF-2012R1A1A2A10041947) and the Global Frontier R&D Program (2013-073298) on Center for Hybrid Interface Materials (HIM) funded by the Ministry of Science, ICT & Future Planning. D.-Y.J. is thankful for the financial support of an NRF grant funded by the Korea government (MEST), 2011-0010905, Pioneer Research Center Program (2010-0019317), and Inha University. Work at Penn State was supported by a National Security Science and Engineering Faculty Fellowship.

■ REFERENCES

(1) Jaffe, B.; Cook, W. R.; Jaffe, H. *Piezoelectric Ceramics*; Academic Press Limited: New York, 1971.

(2) Ahart, M.; Somayazulu, M.; Cohen, R. E.; Ganesh, P.; Dera, P.; Mao, H. K.; Hemley, R. J.; Ren, Y.; Liermann, P.; Wu, Z. Origin of Morphotropic Phase Boundaries in Ferroelectrics. *Nature* **2008**, *451*, 545−548.

(3) Tadmor, E. B.; Waghmare, U. V.; Smith, G. S.; Kaxiras, E. Polarization Switching in $PbTiO_3$: an Ab Initio Finite Element Simulation. *Acta Mater.* **2002**, *50*, 2989−3002.

(4) Akdogan, E. K.; Safari, A. Thermodynamic Theory of Intrinsic Finite-Size Effects in $PbTiO_3$ Nanocrystals. I. Nanoparticle Size-Dependent Tetragonal Phase Stability. *J. Appl. Phys.* **2007**, *101*, 064114.

(5) Yang, Y.; Wang, X.; Sun, C.; Li, L. Stress Induced Curie Temperature Shift in High-Aspect Ratio $PbTiO_3$ Nanotube Arrays. *J. Appl. Phys.* **2008**, *104*, 124108.

(6) Dobal, P. S.; Bhaskar, S.; Majumder, S. B.; Katiyar, R. S. Micro-Raman Investigation of Stress Variations in Lead Titanate Films on Sapphire. *J. Appl. Phys.* **1999**, *86*, 828−834.

(7) Turner, R. C.; Fuierer, P. A.; Newnham, R. E.; Shrout, T. R. Materials for High Temperature Acoustic and Vibration Sensors: A review. *Appl. Acoust.* **1994**, *41*, 299−324.

(8) Tomsia, A. P., Glaeser, A., Eds. *Ceramic Microstructure: Control at the Atomic Level*; Plenum Press: New York, 1998.

(9) Maiwa, H.; Ichinose, N.; Okazaki, K. Preparation and Properties of Ru and RuO_2 Thin Film Electrodes for Ferroelectric Thin Films. *Jpn. J. Appl. Phys.* **1994**, *33*, 5223−5226.

(10) Desu, S. B. Stress Induced Modifications in Ferroelectric Films. *Phys. Status Solidi A* **1994**, *141*, 119−133.

(11) Okazaki, K.; Nagata, K. Effects of Grain Size and Porosity on Electrical and Optical Properties of PLZT Ceramics. *J. Am. Ceram. Soc.* **1973**, *56*, 82−86.
(12) Takahashi, M. Space Charge Effect in Lead Zirconate Titanate Ceramics Caused by the Addition of Impurities. *Jpn. J. Appl. Phys.* **1970**, *9*, 1236−1246.
(13) Sun, C. Q.; Zhong, W. H.; Li, S.; Tay, B. K.; Bai, H. L.; Jiang, E. Y. Coordination Imperfection Suppressed Phase Stability of Ferromagnetic, Ferroelectric, and Superconductive Nanosolids. *J. Phys. Chem. B* **2004**, *108*, 1080−1084.
(14) Fong, D. D.; Kolpak, A. M.; Eastman, J. A.; Streiffer, S. K.; Fuoss, P. H.; Stephenson, G. B.; Thompson, C.; Kim, D. M.; Choi, K. J.; Eom, C. B.; Grinberg, I.; Rappe, A. M. Stabilization of Monodomain Polarization in Ultrathin $PbTiO_3$ Films. *Phys. Rev. Lett.* **2006**, *96*, 127601.
(15) Rossetti, G. A.; Cross, L. E.; Kushida, K. Stress Induced Shift of the Curie Point in Epitaxial $PbTiO_3$ Thin Films. *Appl. Phys. Lett.* **1991**, *59*, 2524−2526.
(16) Samara, G. A. The Relaxational Properties of Compositionally Disordered ABO_3 Perovskites. *J. Phys.: Condens. Matter* **2003**, *15*, R367−R401.
(17) Samara, G. A. Pressure and Temperature Dependence of the Dielectric Properties and Phase Transitions of the Ferroelectric Perovskites: $PbTiO_3$ and $BaTiO_3$. *Ferroelectrics* **1971**, *2*, 277−289.
(18) Schlom, D. G.; Chen, L. Q.; Eom, C. B.; Rabe, K. M.; Streiffer, S. K.; Triscone, J. M. Strain Tuning of Ferroelectric Thin Films. *Annu. Rev. Mater. Res.* **2007**, *37*, 589−626.
(19) Akedo, J. Room Temperature Impact Consolidation (RTIC) of Fine Ceramic Powder by Aerosol Deposition Method and Applications to Microdevices. *J. Therm. Spray Technol.* **2008**, *17*, 181−198.
(20) Ryu, J.; Park, D. S.; Hahn, B. D.; Choi, J. J.; Yoon, W. H.; Kim, K. Y.; Yun, H. S. Photocatalytic TiO_2 Thin Films by Aerosol-Deposition: From Micron-Sized Particles to Nano-Grained Thin Film at Room Temperature. *Appl. Catal., B: Environ.* **2008**, *83*, 1−7.
(21) Ryu, J.; Choi, J. J.; Hahn, B. D.; Park, D. S.; Yoon, W. H.; Kim, K. H. Fabrication and Ferroelectric Properties of Highly Dense Lead-Free Piezoelectric$(K_{0.5}Na_{0.5})NbO_3$ Thick Films by Aerosol Deposition. *Appl. Phys. Lett.* **2007**, *90*, 152901.
(22) Han, G.; Ryu, J.; Yoon, W. H.; Choi, J. J.; Hahn, B. D.; Kim, J. W.; Park, D. S.; Ahn, C. W.; Priya, S.; Jeong, D. Y. Stress-Controlled $Pb(Zr_{0.52}Ti_{0.48})O_3$ Thick Films by Thermal Expansion Mismatch between Substrate and $Pb(Zr_{0.52}Ti_{0.48})O_3$ Film. *J. Appl. Phys.* **2011**, *110*, 124101.
(23) Uchino, K.; Sadanaga, E.; Hirose, T. Dependence of the Crystal Structure on Particle Size in Barium Titanate. *J. Am. Ceram. Soc.* **1989**, *72*, 1555−1558.
(24) Uchino, K.; Sadanaga, E.; Oonishi, K.; Yamamura, H. *Ceramic Dielectrics-Ceramic Transactions*; American Ceramic Society: Westerville, 1990; Vol. *8*, p 107.
(25) Ishikawa, K.; Yoshikawa, K.; Okada, N. Size Effect on the Ferroelectric Phase Transition in $PhTiO_3$ Ultrafine Particles. *Phys. Rev. B* **1988**, *37*, 5852−5855.
(26) Zhong, W. L.; Wang, Y. G.; Zhang, P. L.; Qu, B. D. Phenomenological Study of the Size Effect on Phase Transitions in Ferroelectric Particles. *Phys. Rev. B* **1994**, *50*, 698−703.
(27) De Groot, F. M. F.; Fuggle, J. C.; Thole, B. T.; Sawatzky, G. A. $L_{2,3}$ X-Ray-Absorption Edges of d^0 Compounds: K^+, Ca^{2+}, Sc^{3+}, and Ti^{4+} in O_h (Octahedral) Symmetry. *Phys. Rev. B* **1990**, *41*, 928−937.
(28) Sefat, A. S.; Amow, G.; Wu, M. Y.; Botton, G. A.; Greedan, J. E. High-Resolution EELS Study of the Vacancy-Doped Metal/Insulator System, $Nd_{1-x}TiO_3$, x = 0 to 0.33. *J. Solid State Chem.* **2005**, *178*, 1008−1016.
(29) Torres-Pardo, A.; Gloter, A.; Zubko, P.; Jecklin, N.; Lichtensteiger, C.; Colliex, C.; Triscone, J. M.; Stéphan, O. Pectroscopic Mapping of Local Structural Distortions in Ferroelectric $PbTiO_3/SrTiO_3$ Superlattices at the Unit-Cell Scale. *Phys. Rev. B* **2011**, *84*, 220102.
(30) Eberg, E.; Van Helvoort, A. T. J.; Takahashi, R.; Gass, M.; Mendis, B.; Bleloch, A.; Holmestad, R.; Tybell, T. Electron Energy Loss Spectroscopy Investigation of Pb and Ti Hybridization with O at the $PbTiO_3/SrTiO_3$ Interface. *J. Appl. Phys.* **2011**, *109*, 034104.
(31) Fu, L. F.; Welz, S. J.; Browning, N. D.; Kurasawa, M.; McIntyre, P. C. Z-Contrast and Electron Energy Loss Spectroscopy Study of Passive Layer Formation at Ferroelectric $PbTiO_3$/Pt interfaces. *Appl. Phys. Lett.* **2005**, *87*, 262904.
(32) Kourkoutis, L. F.; Xin, H. L.; Higuchi, T.; Hotta, Y.; Lee, J. H.; Hikita, Y.; Schlom, D. G.; Hwang, H. Y.; Muller, D. A. Atomic-Resolution Spectroscopic Imaging of Oxide Interfaces. *Philos. Mag.* **2010**, *90*, 4731−4749.
(33) Egoavil, R.; Tan, H.; Verbeeck, J.; Bals, S.; Smith, B.; Kuiper, B.; Rijnders, G.; Koster, G.; Van Tendeloo, G. Atomic Scale Investigation of a $PbTiO_3/SrRuO_3/DyScO_3$ Heterostructure. *Appl. Phys. Lett.* **2013**, *102*, 223106.
(34) Klie, R. F.; Browning, N. D. Atomic Scale Characterization of Oxygen Vacancy Segregation at $SrTiO_3$ Grain Boundaries. *Appl. Phys. Lett.* **2000**, *77*, 3737−3739.
(35) Jia, C. L.; Urban, K. Atomic-Resolution Measurement of Oxygen Concentration in Oxide Materials. *Science* **2004**, *303*, 2001−2004.
(36) Lee, S. Y.; Ko, S. W.; Lee, S.; Trolier-McKinstry, S. Mn-Doped $0.15BiInO_3$-$0.85PbTiO_3$ Piezoelectric Films Deposited by Pulsed Laser Deposition. *Appl. Phys. Lett.* **2012**, *100*, 212905.
(37) Taylor, T. R.; Hansen, P. J.; Acikel, B.; Pervez, N.; York, R. A.; Streiffer, S. K.; Speck, J. S. Impact of Thermal Strain on the Dielectric Constant of Sputtered Barium Strontium Titanate Thin Flms. *Appl. Phys. Lett.* **2002**, *80*, 1978−1980.
(38) Watanabe, H.; Yamada, N.; Okaji, M. Linear Thermal Expansion Coefficient of Silicon from 293 to 1000 K. *Int. J. Thermophys.* **2004**, *25*, 221−236.
(39) Foster, C. M.; Li, Z.; Buckett, M.; Miller, D.; Baldo, P. M.; Rehn, L. E.; Bai, G. R.; Guo, D.; You, H.; Merkle, K. L. Substrate Effects on the Structure of Epitaxial $PbTiO_3$ Thin Films Prepared on MgO, $LaAlO_3$, and $SrTiO_3$ by Metalorganic Chemical-Vapor Deposition. *J. Appl. Phys.* **1995**, *78*, 2607−2622.
(40) Xing, X.; Deng, J.; Zhu, Z.; Liu, G. Solid Solution $Ba_{1-x}Pb_xTiO_3$ and its Thermal Expansion. *J. Alloys Compd.* **2003**, *353*, 1−4.
(41) Chen, J.; Xing, X.; Sun, C.; Hu, P.; Yu, R.; Wang, X.; Li, L. Zero Thermal Expansion in $PbTiO_3$-Based Perovskites. *J. Am. Chem. Soc.* **2008**, *130*, 1144−1145.
(42) Tuttle, B.; Headley, T.; Drewien, C.; Michael, J.; Voigt, J.; Garino, T. Comparison of Ferroelectric Domain Assemblages in $Pb(Zr,Ti)O_3$ Thin Films and Bulk Ceramics. *Ferroelectrics* **1999**, *221*, 209−218.
(43) Wang, Z.; Miao, J. Critical Electrode Size in Measurement of d_{33} Coefficient of Films via Spatial Distribution of Piezoelectric Displacement. *J. Phys. D: Appl. Phys.* **2008**, *41*, 035306.